Wu *et al. J Wood Sci* (2019) 65:38
https://doi.org/10.1186/s10086-019-1816-2

Journal of Wood Science

ORIGINAL ARTICLE

Open Access

Mechanical performance of mortise and tenon joints pre-reinforced with slot-in bamboo scrimber plates

Guofang Wu[1,2], Meng Gong[3], Yingchun Gong[1,2], Haiqing Ren[1,2] and Yong Zhong[1,2*]

Abstract

This study was aimed at examining the mechanical performance of mortise and tenon joints reinforced with slot-in bamboo scrimber plates. 27 full-scale specimens were manufactured with engineered wood and bamboo products using computer numerically controlled (CNC) technology, then they were tested under monotonic loading. The initial stiffness and moment carrying capacity of joints with different reinforcing configurations were obtained from the established moment–rotational angle relationships. It was found that the initial stiffness of the reinforced mortise and tenon joints increased by 11.4 to 91.8% and the moment carrying capacity increased by 13.5 to 41.7%, respectively. The total width and grain orientation of the reinforcing plates had significant influence on the mechanical performance of the mortise and tenon joints. Fastening the plates to tenon with dowels was beneficial to the mechanical performance of the joints. The embedment length and adhesive type had no significant influence to the structural performance of the joints. This study demonstrated the feasibility of pre-reinforcing mortise and tenon joints in new timber construction, and could assist to promote the application of mortise and tenon joints in modern timber structures.

Keywords: Mortise and tenon joint, Pre-reinforcement, Mechanical performance, Bamboo scrimber, Beam to column connection

Introduction

A mortise and tenon joint consists of a tongue that inserts into a mortise cut in the mating piece of timber. As one of the oldest joinery methods used in timber structures since at least 7000 years ago [1], its formation and configuration have been in a long process of trial and error [2]. Until the middle of the 20th century, the mortise and tenon joint was still designed and manufactured in terms of the experience of carpenters [3]. Fabrication of the mortise and tenon joint was also rather labor-intensive and prohibitively complicated in comparison with other modern connection methods [4]. As a result, the mortise and tenon joint was once thought inappropriate in the construction of modern timber structures. However, with the development of computer numerically controlled (CNC) manufacturing technology in the late 20th century, the cost-effectiveness of mortise and tenon joint was re-established. With the round timber being replaced by modern engineered wood products like glue-laminated timber (glulam), laminated veneer lumber (LVL), etc., not only the dimension is more accurate, but also the mechanical performance of the joint is more reliable. This joinery method is reviving in wood construction industry [5] and has been used in timber structures like heavy timber buildings again [6]. It is believed that mortise and tenon joint will play an important role in modern industrialized timber structures.

There are a wide variety of mortise and tenon joints [7]. No matter how complex a mortise and tenon joint is, it can always break down into some basic types. The most common one is the straight mortise and tenon joint, whose tenon tongue and mortise hole are both rectangular. As shown in Fig. 1, the moment acting on the straight

*Correspondence: zhongy@caf.ac.cn
[2] Research Institute of Wood Industry, Chinese Academy of Forestry, Beijing 100091, People's Republic of China
Full list of author information is available at the end of the article

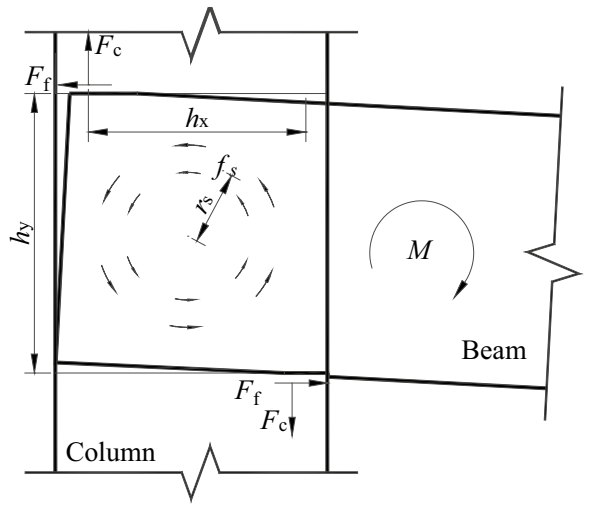

Fig. 1 Sketch of the force and deformation in a straight tenon–mortise joint

mortise and tenon joint is carried by the contact force F_c between tenon tongue and mortise, friction F_f on top and bottom surfaces, and friction F_s on side surfaces. Because the modulus of elasticity of wood in its perpendicular-to-grain direction is significantly lower than that in its parallel-to-grain direction [8], very large perpendicular compressive deformation is induced in tenon by the contact force, and the mortise and tenon joints are usually very ductile [9]. The mortise and tenon joint transfers moment between beam and column in a semi-rigid manner [10, 11]. Research showed that the mechanical performance of mortise and tenon connected timber frame is governed by the behavior of mortise and tenon joints [11, 12]. The mechanical performance of the mortise and tenon connected timber frame can be improved if the strain and stress perpendicular to grain are reduced by appropriate reinforcing methods.

Efforts have been made to investigate the reinforcement of the mortise and tenon joint; however, many of them were focused on reinforcing the joints in historical structures [2, 13–15]. The idea of pre-reinforcement has been applied to other timber joints. For example, both Lam et al. [16] and Gehloff et al. [17] tried to improve the perpendicular to grain properties of wood in bolted timber connections. Recent research on cross-laminated timber (CLT) showed that by assembling the lamination perpendicular to one another, CLT members could have better properties in perpendicular-to-wood-grain direction [18]. Blaß et al. [19] introduced this concept into bolted glulam butt joint connections and found that it improved the performance excellently. Wang et al. [20] pre-reinforced the bolted column joints with locally cross-laminated glulam members and found that the reinforcement method was effective. However, there is still no research about the pre-reinforcement of mortise and tenon joints in new wood construction. In this study, the concept of locally cross-lamination was applied to mortise and tenon joints to improve the perpendicular-to-grain performance. The tenon was pre-reinforced with slot-in bamboo scrimber plates to enhance the mechanical performance of the mortise and tenon joints.

Materials and methods

Materials and specimens

The beam and column were glulam members manufactured with finger-joint-free laminations from No. 1 Canadian Douglas fir dimension lumber, respectively. The physical and mechanical properties of the wood product are listed in Table 1, where the ultimate compression strength properties parallel and perpendicular to grain were determined from full-scale specimens.

Bamboo scrimber is an innovative bamboo-based product that was improved by Yu and Yu [21] and has been popularized in China in the past decades. More information about the fabrication, material properties, and application of the bamboo scrimber was introduced in [22]. Bamboo scrimber was chosen as the reinforcing material because its strength and moduli are higher than wood. The physical and mechanical properties of bamboo scrimber used in this study were determined from small specimens, whose sizes were similar to the small clear specimens of wood. These properties are listed in Table 2.

Two kinds of adhesives provided by local suppliers were used to glue the reinforcing plates, one-component polyurethane resin (PUR) and modified epoxy resin (EPOXY).

As shown in Fig. 2, the T-shaped mortise and tenon joint specimen was an assembly with a beam and

Table 1 Material properties of Douglas fir (average)

E_0 (MPa)	E_{90} (MPa)	G_{12} (MPa)	G_{23} (MPa)	Nu_{12}	Nu_{23}	$f_{t,0}$ (MPa)	$f_{t,90}$ (MPa)	$f_{c,0}$ (MPa)	$f_{c,90}$ (MPa)	S_0 (MPa)
12,360	682	910	213	0.36	0.42	98.4	1.5	46.0	3.3	9.2

E_0 and E_{90} are the longitudinal and transverse modulus of elasticity, respectively. G_{12} and G_{23} are the longitudinal and rolling shear modulus, respectively. Nu_{12} and Nu_{23} are Poisson's ratios. $f_{t,0}$ and $f_{t,90}$ are tensile strength parallel and perpendicular to grain, respectively. $f_{c,0}$ and $f_{c,90}$ are compression strength parallel and perpendicular to grain, respectively. S_0 is the shear strength parallel to grain

Table 2 Material properties of bamboo scrimber (average)

$f_{c,0}$ (MPa)	$f_{c,90}$ (MPa)	$f_{t,0}$ (MPa)	$f_{t,90}$ (MPa)	S_0 (MPa)	E_0 (GPa)	ρ (g/cm^3)
73.46	12.75	112.78	3.73	52.41	16.31	1.11

$f_{c,0}$ and $f_{c,90}$ are compression strength parallel and perpendicular to grain, respectively. $f_{t,0}$ and $f_{t,90}$ are tensile strength parallel and perpendicular to grain, respectively. S_0 is the shear strength parallel to grain. E_0 is the longitudinal modulus of elasticity and ρ the density

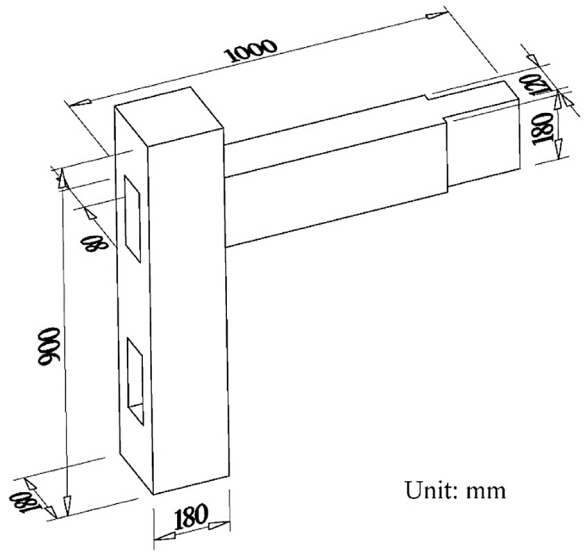

Fig. 2 Mortise and tenon joint specimen

column. The dimensions of the column were 180 mm in width, 180 mm in depth, and 900 mm in length, while the dimensions of the beam were 120 mm in thickness, 180 mm in depth, and 1000 mm in length. To efficiently use the materials, two 80 × 180 mm mortises were carved through the column and a tenon tongue with the same dimension was processed at each end of a beam. Thus, one beam and one column can be used to make two joints, with each tenon and mortise being used only once. Slots were cut in the tenon tongue to accommodate the reinforcing bamboo scrimber plates. All the carpentry work was done by the Joinery Machine K2i (Hundegger), except that the filet corner of the mortise was manually trimmed.

The bamboo scrimber panels were processed into 10-mm-thick plates with aimed dimension. After the adhesive applied, the plates were inserted into the slots cut in the tenon. Then, the beam was cured in a chamber for 2 weeks with two steel clamps pressing the tenon and reinforcing plates tightly. As shown in Fig. 3, there were two reinforcing plates in both Patterns *i* and *ii* while three reinforcing plates in Pattern *iii*. The Pattern *ii* resulted in a 20/10/20/10/20-mm layup in the tenon region. The grain of bamboo scrimber may be arranged parallel or perpendicular to the wood grain. Moreover, steel dowels were installed in some tenons. Two 16-mm-diameter dowels were made with Q335 steel [23] and embedded into the tenon at a 30 mm edge and end distance. The dowels were used to avoid cracking in the tenon by mitigating the shear stress in wood. The dowels were installed only in the lower end and upper

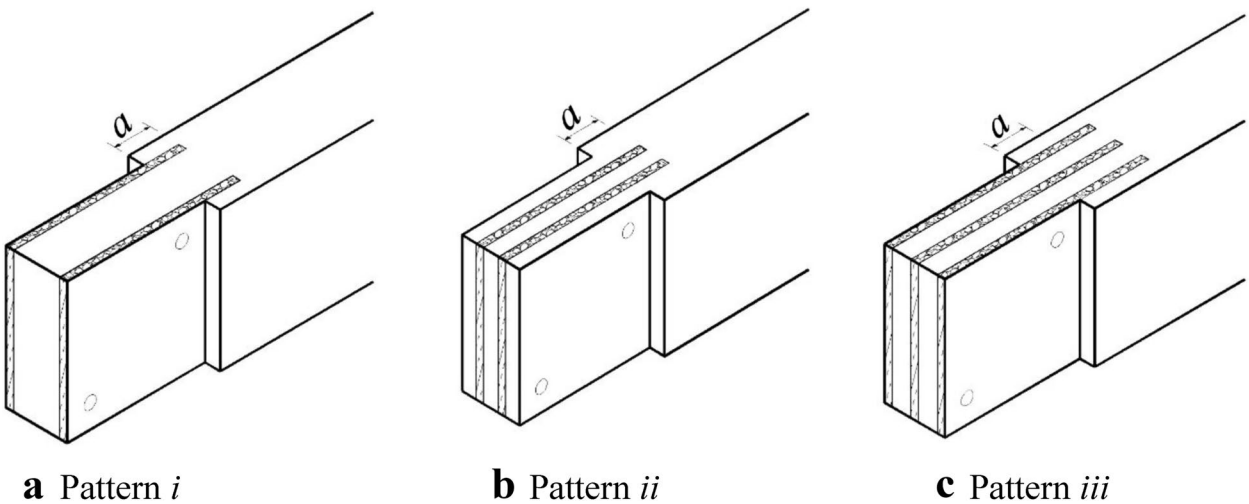

Fig. 3 Reinforcing methods of tenon

root of the tenon. As the joints were loaded monotonically, the dowels located as far as possible away from the action point of the force that they can carry all of the forces in the part of plates above the dowel. And the edge and end distance were chosen to avoid local fracture in wood. The beam was installed to the column with the dowel at the end placed downwardly.

In this study, 27 specimens of mortise and tenon joints were manufactured. The specimens in the control group C1 were straight through mortise and tenon joints without any reinforcement, while the tenons in other groups were reinforced with bamboo scrimber plates with different configurations including pattern of slots, grain of bamboo scrimber, adhesive types and whether dowels applied. The configuration of each test group is listed in Table 3.

Methods

As illustrated in Fig. 4, the column was fixed to the reaction frame by constraining the horizontal and vertical displacements at both ends. At each end of column, one thick steel plate was fastened to the reaction frame with 2 anchor bolts which pressed the column tightly to the reaction frame. Two rib-stiffened steel arms were used to clamp the column from top and bottom ends, and some thin steel plates were inserted into the gap between the upper arm and top end of the column to prevent vertical rigid body movement. The vertical load was applied to the free end of the beam via a steel cage hooked around the beam and away from the tenon. The cage was hinged to an MTS actuator (MTS Systems Corporation, USA), which was anchored to a portal reaction frame with a ball hinge.

Table 3 Configuration of specimens in each test group

Group ID	Replicates	Plate configurations			Connection between plates and tenon	
		a^*/mm	Pattern	Grain	Adhesive type	With dowel
C1	6	–	–	–	–	–
B-*i*-//-E	3	50	*i*	//	EPOXY	No
B-*i*-//-D-E	3	50	*i*	//	EPOXY	Yes
B-*i*-//-D-P	3	50	*i*	//	PUR	Yes
B-*i*-⊥-D-P	3	100	*i*	⊥	PUR	Yes
B-*ii*-⊥-D-E	3	50	*ii*	⊥	EPOXY	Yes
B-*ii*-⊥-D-E0	3	0	*ii*	⊥	EPOXY	Yes
T-*iii*-⊥-D-E	3	100	*iii*	⊥	EPOXY	Yes

a is the length of the reinforcing plates extended into the beam beyond the tenon shoulder

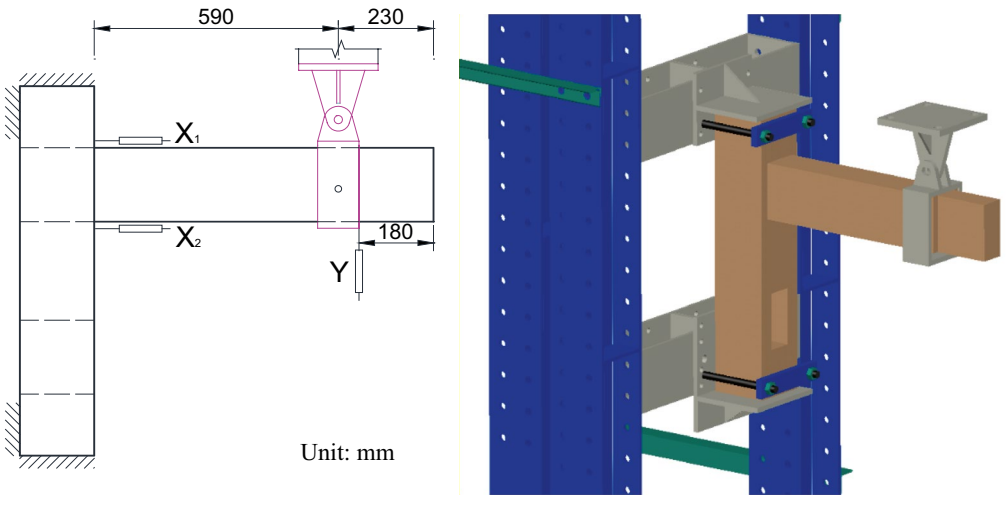

a 2D drawing **b** 3D illustration

Fig. 4 Schematic of the test setup

The loading capacity of the actuator was 250 kN and the stroke range was 250 mm. The loading rate was 8 mm/min, i.e., the crosshead movement. The joints were loaded to failure or when the actuator reached the stroke limit.

The load applied by the actuator was measured by a build-in load cell, and the relative displacements between beam and column were measured by two displacement transducers denoted by X1 and X2 horizontally mounted on top and bottom surface of the beam, respectively. Besides, the vertical displacement of the beam was measured by a transducer denoted by Y as well. The outputs of the X1 and X2 were used for the subsequent computations of rotational angle, and the output of Y served as a reference for result checking. All data, including load and displacements, were recorded by the data logger TDS530 (Tokyo Sokki Kenkyujo Co., Japan) at a frequency of 1 Hz.

Results and discussion

Failure modes

Unreinforced joints

With the increasing vertical load, the beam rotated about the rotation center. As shown in Fig. 5, for the unreinforced joints, the upper surface of the end part of the tenon was pressed to the mortise tightly, and perpendicular-to-grain compressive deformation was observed in the tenon end; meanwhile, the bottom surface of tenon gradually separated with the mortise. Moreover, the upper end of tenon had the trend of withdrawing from the mortise, but the tenon did not separated with the mortise.

The joints were disassembled after test to check the deformation and fracture in tenon tongue and mortise. Considerable perpendicular-to-grain compressive deformation was observed at two locations: the upper surface of tenon at the end and the bottom surface of the tenon near the shoulder, indicating that the contact forces in these two regions were critical. Besides, there was a crack sighted at the lower section of tenon in some specimens, which might be caused by the perpendicular-to-grain tensile stress that balanced the compressive stress near the shoulder. There was no obvious deformation found inside the mortise hole; however, local compressive traces were found in column at the contact area between beam shoulder and column.

Reinforced joints

For the reinforced joints, besides withdrawing and separation of the tenon with the mortise, different kinds of cracks were observed at the end of tenons during the loading process, as shown in Fig. 6. For specimens in

Fig. 5 Failure mode of the unreinforced mortise and tenon joint (specimen C1–2)

a B-*i*-//-E **b** B-*i*-//-D-P **c** B-*ii*-⊥-D-E

Fig. 6 Cracks observed in the reinforced mortise and tenon joints

group B-*i*-//-E, whose reinforcing plates were glued then to the tenon without dowel, the tenon vertically cracked. This was because the MOE of reinforcing plate was much higher than wood, and thus, they absorbed more contact forces than wood. There were force differences between the reinforcing plates and beam, which caused shear stress distributed in the glue line and within wood near the glue line. As the rolling shear strength of wood was too small to undertake the shear stress, thus the wood cracked. However, in reinforced joints where dowels were added, this kind of failure was not found. Horizontal cracks were sighted in bamboo scrimber plates in tenons where the reinforcing plates were placed parallel to the tenon grain; however, there was no horizontal crack in the perpendicularly placed bamboo scrimber plates, because the parallel-to-grain tensile strength was much higher than the perpendicular-to-grain strength for bamboo scrimber. In almost all of the specimens, there was no crack in the glue line between bamboo scrimber and tenon, indicating that the bond strength of both adhesives was good.

The joints were dismantled after the tests. As shown in Fig. 7, the excessive perpendicular-to-grain compressive deformation of tenon was significantly reduced due to the presence of reinforcing plates. For tenons reinforced with bamboo scrimber plates in parallel or perpendicular to the tenon, the reinforcing plates did not deform simultaneously with the wood. Although the wooden part of tenon still underwent rather large compressive deformation, there was nearly no obvious compressive deformation sighted in the reinforcing plates. For the reinforced tenon with perpendicularly plated scrimber plates, it was also found that the bamboo scrimber cracked perpendicular to grain. The cracks were caused by the horizontal frictional force, which applied on the upper surface

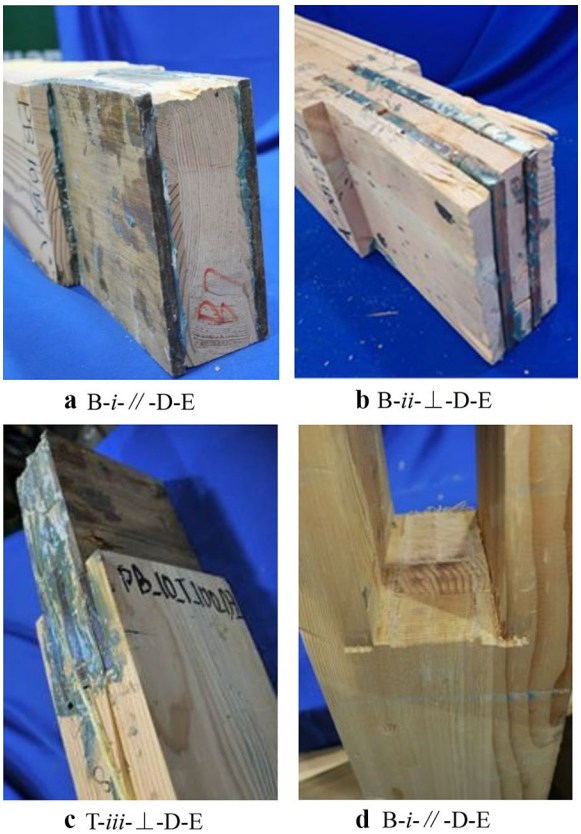

a B-*i*-//-D-E **b** B-*ii*-⊥-D-E

c T-*iii*-⊥-D-E **d** B-*i*-//-D-E

Fig. 7 Failure modes of the reinforced mortise and tenon joints

of the tenon and produced perpendicular-to-grain tension stress in the reinforcing plates. For the tenons where reinforcing plates extended 100 mm into the beam, i.e., the groups B-*i*-⊥-D-P and T-*iii*-⊥-D-E, bending failure was found in the beam, suggesting that the reinforcing plates worked well with the tenon as a whole.

For the reinforced joints, it was found that strip-like traces were found in the mortise hole at the corresponding position of the reinforcing plates. This was because the bamboo scrimber was much stronger than wood.

Results and analysis

Curves and data

The intersection of the neutral axes of beam and column was assumed as the center of rotation. The moment was generated by the applied vertical load with respect to the rotation center. And the rotational angle was calculated from the two horizontal transducers. The moment–rotational angle curves of specimens in each test group were averaged and shown in Fig. 8. For the reinforced joints, the peak load was reached before 0.10 rad, but for the unreinforced joints, the load could keep increasing until the actuator's limits were reached. However, it should be noted that in practice the rotational angle of mortise and tenon joints could not generally exceed 0.1 rad, at which the horizontal drift of a 3-m-high column could reach about 300 mm.

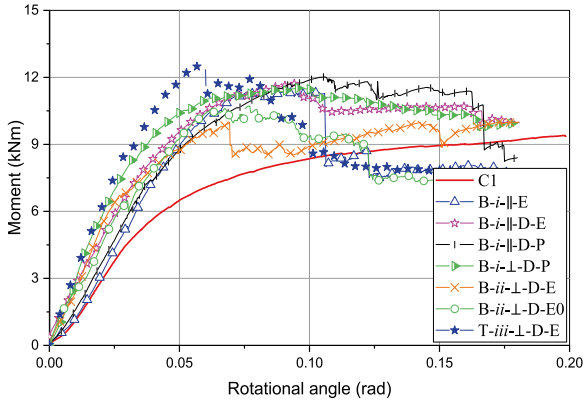

Fig. 8 Average moment–rotational angle curves of each group

It clearly shows that the specimens of control group C1 (no reinforcement) exhibited lower stiffness. The slot-in plates reinforcing mortise and tenon joints created completely stiffer and stronger joints than the unreinforced joints. The loads carried by the unreinforced joints kept increasing without obvious peak and it seemed that they carried more load than some reinforced joints when rotational angle was large enough. But as stated above, in practical the mortise and tenon joints were not allowed to undergo such large rotational angle.

The moment carrying capacity of the joints was determined based on the peak point (or the ultimate point in case no failure occurred) of the moment–rotational angle curves. Then, the portion of curve ranging between 15 and 40% (this range was subjected to slight change if apparent nonlinearity was observed in this portion) of the peak moment was fitted with a linear function to find the initial stiffness. The average and coefficient of variation (COV) of moment carrying capacity and the initial stiffness of specimens in one group were determined and listed in Table 4. And the reinforcing effect was evaluated with the index of increasing rate of reinforced joints to the unreinforced joints for both moment carrying capacity and initial stiffness. These two rates are listed in Table 4 as well.

Discussion

As listed in Table 4, the initial stiffness of the reinforced mortise and tenon joints increased by 11.4 to 91.8% and the moment carrying capacity increased by 13.5 to 41.7% in different reinforcing configurations. This indicated that the proposed reinforcing method was an effective way to enhance the mechanical performance of the mortise and tenon joints.

The COV of the initial stiffness of the mortise and tenon joints with bamboo scrimber plates placed in parallel to the tenon was lower than that of joints with

Table 4 Moment carrying capacity and initial stiffness of each test group

Group ID	Moment carrying capacity		Initial stiffness		Increasing rate (%)	
	Average (kN m)	COV	Average (kN m/rad)	COV	Moment	Stiffness
C1	9.37	0.05	189.58	0.12	–	–
B-*i*-//-E	11.96	0.20	211.18	0.03	27.6	11.4
B-*i*-//-D-E	12.20	0.05	245.98	0.09	30.3	29.7
B-*i*-//-D-P	12.30	0.18	227.30	0.03	31.3	19.9
B-*i*-⊥-D-P	11.55	0.07	356.24	0.24	23.3	87.9
B-*ii*-⊥-D-E	10.64	0.12	269.54	0.11	13.5	42.2
B-*ii*-⊥-D-E0	11.10	0.28	355.02	0.45	18.4	87.3
T-*iii*-⊥-D-E	13.28	0.18	363.71	0.35	41.7	91.8

bamboo scrimber plates placed perpendicular to the tenon. Because in perpendicularly placed bamboo scrimber plates, vertical cracks took place, which introduced non-uniformly distributed stress in the bamboo scrimber plates and caused different influences on the frictional force between the tenon and mortise in different specimens.

Effect of dowel Both the moment carrying capacity and initial stiffness of joints in B-*i*-//-D-E were larger than those of the B-*i*-//-E, indicating that the presence of mechanical fasteners provided a positive effect on the structural performance of the mortise and tenon joints.

Effect of adhesive type Adhesive type was the only different factor in groups B-*i*-//-D-E and B-*i*-//-D-P. By ANOVA (analysis of variation) analysis, it was found that the adhesives used in this study had no significant contribution to the mechanical performance of the mortise and tenon joints. This agreed well with the phenomenon that no glue line failure was observed in joints with either adhesive. Thus, further analysis was performed without taking the adhesive type into account.

Effect of embedment length The influence of the embedment length (denoted by "*a*" as shown in Fig. 3) of the reinforcing plates can be investigated by comparing the moment carrying capacity and initial stiffness of groups B-*ii*-⊥-D-E0, B-*ii*-⊥-D-E, whose extension length was 0 and 50 mm, respectively. ANOVA analysis was performed to compare the difference and it was found that the embedment length actually had no significant influence on the moment carrying capacity and initial stiffness to the joints at the significant level of 0.05. This could be explained based on the experimental observations that deformation of the joint was localized to the tenon; the effect of increasing the embedment length to the mechanical performance was marginal.

Effect of grain mode As the embedment length had no significant influence on the mechanical performance of the mortise and tenon joints, ANOVA analysis was performed to compare the moment carrying capacity and initial stiffness of joints in groups B-*i*-⊥-D-P and B-*i*-//-D-P. At the significant level of 0.05, there was no significant difference between moment carrying capacity of joints with different grain orientation. However, the probability that the initial stiffnesses were identical for joints with different grain orientation was only 6.6%, suggesting that the grain orientation had a considerable influence on the initial stiffness if taking the limited specimen number into account.

Effects of slot pattern Although the location of plates was different in slot patterns *i* and *ii*, but the total width was the same; however, the total width of the plates was larger than both slot patterns *i* and *ii*. ANOVA analysis was performed to compare the moment carrying capacity and initial stiffness of joints in groups B-*i*-⊥-D-P and B-*ii*-⊥-D-E. It was found that there was no significant difference between the slot patterns *i* and *ii* of both moment carrying capacity and initial stiffness, indicating that the location of slots has no significant influence to the mechanical performance if the replacing rate was the same.

Then ANOVA analysis was performed to compare the moment carrying capacity and initial stiffness of joints in groups B-*i*-⊥-D-P and T-*iii*-⊥-D-E, both the carrying capacity and initial stiffness were significantly different for these two groups. And both the moment carrying capacity and initial stiffness were the largest in all test configurations for joints in group T-*iii*-⊥-D-E, indicating that the more the wood was replaced, the better the structural performance of the mortise and tenon joints was, at least below the replacing rate of 3/8.

Conclusions

The method of reinforcing the mortise and tenon joints with slot-in bamboo scrimber plates was developed and the effect of different configurations on the initial stiffness and moment carrying capacity was experimentally investigated. The main conclusions could be drawn as follows:

(1) Both the capacity and stiffness could be effectively increased by the proposed slot-in bamboo scrimber plates pre-reinforcing method. Within the range of parameters investigated, the stiffness of the reinforced mortise and tenon joints was increased by 11.4 to 91.8% and the moment carrying capacity was increased by 13.5 to 41.7%.
(2) The total width and grain orientation of the reinforcing plates had significant influence on the mechanical performance of the mortise and tenon joints. Both adhesives were interchangeable because failure does not happen in the glue line. There was no obvious influence by extending the reinforcing plates beyond the shoulder into the beam. And the presence of mechanical fasteners provided a positive effect on the mechanical performance of the mortise and tenon joints.

Abbreviations
CNC: computer numerical control; LVL: laminated veneer lumber; F_c: contact force; F_f: friction on top and bottom surfaces; F_s: friction on side surfaces; CLT: cross-laminated timber; E_0: longitudinal modulus of elasticity; E_{90}: transverse modulus of elasticity; G_{12}: longitudinal shear modulus; G_{23}: rolling shear modulus; Nu_{12}: Poisson's ratio; Nu_{23}: Poisson's ratio; $f_{t,0}$: tensile strength parallel to grain; $f_{t,90}$: tensile strength perpendicular to grain; $f_{c,0}$: compression strength parallel to grain; $f_{c,90}$: compression strength perpendicular to grain; S_X: shear strength parallel to grain; ρ: density; PUR: one-component polyurethane resin; EPOXY: modified epoxy resin; MOE: modulus of elasticity; COV: coefficient of variance; ANOVA: analysis of variation.

Acknowledgements
The authors are grateful for the financial support from Fundamental Research Funds of Research Institute of Forestry New Technology, CAF (Grant No. CAFYBB2017SY036) and the New Brunswick Innovation Foundation (Canada) under its New Brunswick Research Innovation Chair Program.

Authors' contributions
GW designed the study and wrote the manuscript. GW, YG and HR performed the research and analyzed data. YZ and MG supervised the project. All authors read and approved the final manuscript.

Funding
This study was supported by Fundamental Research Funds of Research Institute of Forestry New Technology, CAF (CAFYBB2017SY036), "Structural performance of typical tenon–mortise joints and reinforcing" and New Brunswick Innovation Foundation (Canada) under its New Brunswick Research Innovation Chair Program.

Availability of data and materials
The datasets used or analyzed during the current study are available from the corresponding author on reasonable request.

Competing interests
The authors declare that they have no competing interests.

Author details
[1] Research Institute of Forestry New Technology, Chinese Academy of Forestry, Beijing 100091, People's Republic of China. [2] Research Institute of Wood Industry, Chinese Academy of Forestry, Beijing 100091, People's Republic of China. [3] Wood Science and Technology Centre, University of New Brunswick, Fredericton, Canada.

Received: 12 March 2019 Accepted: 18 July 2019
Published online: 26 July 2019

References

1. Tegel W, Elburg R, Hakelberg D, Stäuble H, Büntgen U (2012) Early neolithic water wells reveal the world's oldest wood architecture. PLoS ONE 7(12):e51374. https://doi.org/10.1371/journal.pone.0051374
2. Branco JM, Descamps T (2015) Analysis and strengthening of carpentry joints. Constr Build Mater 97:34–47. https://doi.org/10.1016/j.conbuildmat.2015.05.089
3. Tannert T (2016) Improved performance of reinforced rounded dovetail joints. Constr Build Mater 118:262–267. https://doi.org/10.1016/j.conbuildmat.2016.05.038
4. Ogawa K, Sasaki Y, Yamasaki M (2016) Theoretical estimation of the mechanical performance of traditional mortise–tenon joint involving a gap. J Wood Sci 62(3):242–250. https://doi.org/10.1007/s10086-016-1544-9
5. Tannert T, Prion H, Lam F (2007) Structural performance of rounded dovetail connections under different loading conditions. Can J Civ Eng 34(12):1600–1605. https://doi.org/10.1139/L07-076
6. O'Connell TD, Smith PM (1999) The North American timber frame housing industry. For Prod J 49(1):36–42
7. Chen Z, Zhu E, Lam F, Pan J (2014) Structural performance of Dou-Gong brackets of Yingxian Wood Pagoda under vertical load—an experimental study. Eng Struct 80:274–288. https://doi.org/10.1016/j.engstruct.2014.09.013
8. Descamps T, Léoskool L, Laplume D, Van Parys L, Aira JR (2014) Sensitivity of timber hyper static frames to the stiffness of step and ridge joints. In: Salenikovich A (ed) Proceedings of the 2014 world conference on timber engineering, Quebec
9. Thelandersson S, Larsen HJ (eds) (2003) Timber engineering. Wiley, New York
10. Pang SJ, Oh JK, Park JS, Park CY, Lee JJ (2010) Moment-carrying capacity of dovetailed mortise and tenon joints with or without beam shoulder. J Struct Eng 137(7):785–789. https://doi.org/10.1061/(ASCE)ST.1943-541X.0000323
11. Hanazato T, Fujita K, Sakamoto I, Inayama M, Ohkura Y (2004) Analysis of earthquake resistance of five-storied timber pagoda. In: 13th world conference on earthquake engineering, Vancouver 1–6 August 2004
12. King WS, Yen JR, Yen YA (1996) Joint characteristics of traditional Chinese wooden frames. Eng Struct 18(8):635–644. https://doi.org/10.1016/0141-0296(96)00203-9
13. Parisi MA, Piazza M (2000) Mechanics of plain and retrofitted traditional timber connections. J Struct Eng 126(12):1395–1403. https://doi.org/10.1061/(ASCE)0733-9445(2000)126:12(1395)
14. Sangree RH, Schafer BW (2009) Experimental and numerical analysis of a halved and tabled traditional timber scarf joint. Constr Build Mater 23(2):615–624. https://doi.org/10.1016/j.conbuildmat.2008.01.015
15. Lu W, Deng D (2012) Experimental research on seismic performance of wooden mortise–tenon joints before and after reinforcement (in Chinese). Earthq Eng Eng Vib 32(3):109–116. https://doi.org/10.13197/j.eeev.2012.03.020
16. Lam F, Schulte-Wrede M, Yao CC, Gu, JJ (2008) Moment resistance of bolted timber connections with perpendicular to grain reinforcements. In: Proceedings of the 10th world conference on timber engineering, Miyazaki, 2–5 June 2008
17. Gehloff M, Closen M, Lam F (2010) Reduced edge distances in bolted timber moment connections with perpendicular to grain reinforcements. In: Proceedings of the 2010 world conference on timber engineering, Trentino, 20–24 2010
18. Gagnon S, Pirvu C (eds) (2011) CLT handbook: cross-laminated timber. FPInnovations, Vancouver
19. Blaß HJ, Schädle P (2011) Ductility aspects of reinforced and non-reinforced timber joints. Eng Struct 33(11):3018–3026. https://doi.org/10.1016/j.engstruct.2011.02.001
20. Wang M, Song X, Gu X, Zhang Y, Luo L (2014) Rotational behavior of bolted beam-to-column connections with locally cross-laminated glulam. J Struct Eng 141(4):04014121. https://doi.org/10.1061/(ASCE)ST.1943-541X.0001035
21. Yu W, Yu Y (2013) Manufacturing technology of bamboo-based fiber composites with high-performance (in Chinese). World Bamboo and Rattan 11(3):6–10. https://doi.org/10.3969/j.issn.1672-0431.2013.03.002
22. Yu Y, Zhu R, Wu B, Hu Y, Yu W (2015) Fabrication, material properties, and application of bamboo scrimber. Wood Sci Technol 49(1):83–98. https://doi.org/10.1007/s00226-014-0683-7
23. GB50017 (2017) Code for design of steel structures. Ministry of construction of the People's Republic of China, Beijing

Publisher's Note